




RESEARCH ARTICLE | OCTOBER 30 2023

## On relaxation times of heteroclinic dynamics **FREE**

Special Collection: [Nonlinear dynamics, synchronization and networks: Dedicated to Jürgen Kurths' 70th birthday](#)

Manoj Aravind  ; Hildegard Meyer-Ortmanns  



Chaos 33, 103138 (2023)

<https://doi.org/10.1063/5.0166803>



View  
Online



Export  
Citation

CrossMark



## APL Quantum

Bridging fundamental quantum research with technological applications

**Now Open for Submissions**

No Article Processing Charges (APCs) through 2024

**Submit Today**

# On relaxation times of heteroclinic dynamics

Cite as: Chaos 33, 103138 (2023); doi: 10.1063/5.0166803

Submitted: 7 July 2023 · Accepted: 4 October 2023 ·

Published Online: 30 October 2023 · Corrected: 1 November 2023



View Online



Export Citation



CrossMark

Manoj Aravind<sup>1</sup>  and Hildegard Meyer-Ortmanns<sup>1,2,a)</sup> 

## AFFILIATIONS

<sup>1</sup>School of Science, Constructor University, 28759 Bremen, Germany

<sup>2</sup>Complexity Science Hub Vienna, 1080 Vienna, Austria

**Note:** This paper is part of the Focus Issue on Nonlinear dynamics, synchronization and networks: Dedicated to Juergen Kurths' 70th birthday.

<sup>a)</sup>Author to whom correspondence should be addressed: [hortmanns@constructor.university](mailto:hortmanns@constructor.university)

## ABSTRACT

Heteroclinic dynamics provide a suitable framework for describing transient dynamics such as cognitive processes in the brain. It is appreciated for being well reproducible and at the same time highly sensitive to external input. It is supposed to capture features of switching statistics between metastable states in the brain. Beyond the high sensitivity, a further desirable feature of these dynamics is to enable a fast adaptation to new external input. In view of this, we analyze relaxation times of heteroclinic motion toward a new resting state, when oscillations in heteroclinic networks are arrested by a quench of a bifurcation parameter from a parameter regime of oscillations to a regime of equilibrium states. As it turns out, the relaxation is underdamped and depends on the nesting of the attractor space, the size of the attractor's basin of attraction, the depth of the quench, and the level of noise. In the case of coupled heteroclinic units, it depends on the coupling strength, the coupling type, and synchronization between different units. Depending on how these factors are combined, finite relaxation times may support or impede a fast switching to new external input. Our results also shed some light on the discussion of how the stability of a system changes with its complexity.

Published under an exclusive license by AIP Publishing. <https://doi.org/10.1063/5.0166803>

Heteroclinic dynamics is a suitable framework for transient processes in which the system dwells for a long time in an apparently stable state, but suddenly switches to another state and dwells there again for a while before switching to the next state, often repeatedly. For cognitive and other transient processes in the brain, heteroclinic dynamics is appreciated for reconciling two features that seemed to be incompatible originally: The temporal order of neuronal excitation patterns is well reproducible, but the dynamics is highly sensitive to external input such as sensory one. Some features of the switching statistics of metastable states in the brain can be captured when trajectories in phase space approach heteroclinic connections between saddles, dwelling long in the vicinity of the saddles and switching fast between the saddles, given some fixed input; but beyond a high sensitivity to the input, a desirable attribute of heteroclinic dynamics would be to allow a fast response when the external input changes. To mimic such a sudden change, we measure the time it takes a heteroclinic network (HN) in oscillatory motion to arrest its oscillations when a bifurcation parameter is quenched toward a regime of resting dynamics. As it turns out, the time it takes the system to approach the new resting state depends on the size

of the quench, the nesting of the attractor space, the size of the attractor's basin of attraction, the strength and realization of noise, and the strength and type of coupling to other oscillatory units. The extent to which the oscillations are underdamped will support or impede a fast response to a change in the external input. Our results also shed some light on the discussion of how the stability of a system changes with an increase in its complexity, here referring to systems with nested oscillations and different inherent time scales.

## I. INTRODUCTION

Heteroclinic dynamics provides a framework for intrinsically transient dynamics with very different applications, ranging from applications to ecological systems,<sup>1</sup> hydrodynamics,<sup>2</sup> game theory,<sup>3,4</sup> and, last but not least, to brain dynamics.<sup>5</sup> In particular, it is suited to describe cognitive processes in the brain related to the sequential memory,<sup>6</sup> attention,<sup>7</sup> decision making,<sup>8</sup> binding,<sup>6,9</sup> or chunking.<sup>10</sup>

Heteroclinic dynamics is mapped to heteroclinic networks with nodes, which correspond to saddles, and edges, which are the

heteroclinic connections between the saddles. It should be noticed that heteroclinic networks are networks in phase space. In the simplest case, the saddles are saddle equilibria, and the trajectory of the dynamics approaches the vicinity of saddles, dwells there for some time, depending on the vicinity to the saddle, and then switches to the next saddle. If the trajectory is closed and returns to the vicinity of the first saddle, it approaches a heteroclinic cycle (HC). The revolution of the trajectory needs more and more time to complete, the closer it comes to the heteroclinic cycle. The resulting oscillations are like limit cycles with a well defined period if a suitable strength of noise is present, without noise they are intermittent. In our envisaged application, this means that for a relatively long time, in the vicinity of a saddle, a certain neuronal population is dominant in the excitation pattern; suddenly, it becomes suppressed in favor of another population that becomes dominant for a relatively long time, and the switching goes on between different temporarily dominant populations.

Heteroclinic dynamics was shown to solve an apparent conflict between well reproducible transient dynamics that is robust against noise and, at the same time, very sensitive to external input. Roughly speaking, external input selects the specific heteroclinic sequence, and given such a sequence, the dynamics is dissipative, forgets the initial conditions, and different starting points lead to trajectories in the same channel along the heteroclinic connections of the sequence. The dynamics is competitive between the different states, assigned to the saddles, and realizes the concept of winnerless competition,<sup>1</sup> for which we use an implementation in terms of Generalized Lotka–Volterra (GLV)-equations.

Intrinsically fast are the switches between different saddles, which belong to one and the same sequence. This is a characteristic feature of heteroclinic motion. In addition, if fast adaptation to new external input is required, also the transition to a different sequence or to a resting state should happen fast. This is where relaxation times play a role. For fast adaptation, relaxation times should be small. In our realization in terms of GLV-equations, the external input is not modeled explicitly but assumed to be responsible for the very selection of the itinerary in the network (determined by the choice of competition rates). As a simple option, we model a change of the external input by the attempt to arrest the ongoing oscillations (ongoing either in a single unit or in pacemaker units, as we explain below). We enforce the arrest by a quench in the bifurcation parameter from regimes of oscillatory motion to a regime with resting states, that is, stable equilibria of coexisting subpopulations; we measure the relaxation time as the time it takes the oscillations' amplitudes to decay below a very small threshold (practically indistinguishable from non-oscillatory resting states). Naively, one may expect that such a quench in the bifurcation parameter entails an instantaneous arrest of the oscillations.

This is not the case. As we shall see by numerical simulations, it is the structure and size of the basin of attraction of an attractor that determines how fast a new state (here the resting state) is approached rather than the mere number of types of neuron populations that get excited. To have some nesting in the attractor space, we consider a heteroclinic cycle between three heteroclinic cycles, each of them acting as saddle and realized itself between three saddle equilibria. We measure the relaxation time of such a heteroclinic unit (HU) with two inherent time scales and two levels of

hierarchy as we quench a corresponding bifurcation parameter (the decay rate) from a regime of nested heteroclinic cycles to a regime of resting coexisting “items” in a saddle equilibrium. For a single unit, we compare the relaxation time with systems with no nesting in the attractor space. We measure relaxation times also as a function of the level of noise and the depth of the quench, from points off or close to the bifurcation region. For coupled systems of heteroclinic units on spatial grids, we study the influence of entrainment and synchronization on the duration of relaxation.

As it turns out, large relaxation times are favored by a very low level of noise, by a quench into the vicinity of the bifurcation region, nesting in the attractor space, and a large basin of attraction. In favor of short relaxation times are an intermediate level of noise, a quench which is starting and ending off the bifurcation region, a small basin of attraction, and coupling that leads to strong synchronization.

We consider these numerical simulations only as a first step toward exploring the phenomenology of switching dynamics and involved delay times when bifurcation parameters are quenched between different regimes of the dynamics, here used as an effective description of realizing a change of the external input.

The remainder of the paper is organized as follows. In Sec. II, we summarize some basic notions of heteroclinic dynamics and present the model in its different realizations. Section III A discusses various impacts, such as the strength of noise on the duration of relaxation in a single unit (without spatial coupling to other units). Sections III B and III C deal with relaxation in systems of driven units, entrained by a pacemaker along a chain, and Sec. III D with relaxation when units on a two-dimensional grid synchronize due to diffusive coupling. We conclude with a summary and outlook in Sec. IV.

## II. THE MODEL

Let us first briefly summarize some basic notions of heteroclinic dynamics. For more formal definitions, we refer to the original literature: Early seminal papers on heteroclinic networks are Refs. 11 and 12 (see, for example, also Ref. 13). When the unstable manifold of a saddle equilibrium intersects the stable manifold of another saddle, the intersection is called a heteroclinic orbit. A heteroclinic network (HN) is a set of vertices, corresponding to saddles, connected by edges, which are heteroclinic orbits. As indicated before, saddles in these networks are not restricted to saddle equilibria but refer to any invariant set with non-trivial stable and unstable manifolds. A heteroclinic cycle (HC) between saddle equilibria, in which the unstable direction of one saddle becomes the stable direction of the subsequent saddle, is just a simple special case of a general heteroclinic network.

To study the effect of synchronization, we also couple HNs on a spatial grid, as considered in Ref. 14. To disentangle HNs from network aspects of the spatial grid, we term HNs assigned to a single site of the grid a heteroclinic unit (HU). Thus, the coupling of HUs refers to their coupling in coordinate space. If the HN involves a hierarchy in time scales, we deal with a hierarchical HN or HU (HHN or HHU), respectively.

The system of HUs is defined on regular grid topologies with nodes labeled by  $k$ . To each node, we assign a HU that obeys

GLV-equations. GLV-equations realize the concept of winnerless competition,<sup>15</sup> in which the winners (dominant subpopulations) change over time. For different versions and possible interpretations of sets of GLV-equations, we refer to excellent reviews.<sup>5,7,16–19</sup> Here, we use the following set:

$$\partial_t s_{k,i} = \rho s_{k,i} - \gamma_k s_{k,i}^2 - \sum_{j \neq i} A_{ij} s_{k,i} s_{k,j} + \sum_l K_{k,l} (s_{l,i} - s_{k,i}) + \sigma_k \xi_i(t). \quad (1)$$

In applications to neuronal networks and brain dynamics, we interpret  $s_{k,i}$  as densities of neural subpopulations. During the winnerless competition, a sequence of saddles is approached. In the vicinity of individual saddles, various specific subpopulations get temporarily dominantly excited. Information (for example, from sensory input) is believed to be encoded in the specific spatiotemporal excitation pattern. In the vicinity of a saddle, the variable  $s_{k,i}(t)$  tells us, which subpopulation ( $i$ ) gets dominantly excited, at what location ( $k$ ), and at what time ( $t$ ). In short, we term the variables  $s_{k,i}$  the “items,” without specifying the neural populations any further. Parameter  $\rho$  is the net reproduction rate, chosen as 1 to set the time scale;  $\gamma_k$  alters the net reproduction rate of the  $k$ th unit in an item-density dependent way, and it will serve as a bifurcation parameter;  $\sigma_k$  is the strength of the additive noise to the  $k$ th unit, and  $\xi$  is Gaussian white noise with zero mean.  $A$  is the rate matrix, with  $A_{ij}$  being the competition rate with which item  $j$  of a unit acts on item  $i$  of the same unit. Note the sign in front of  $A_{ij}$  such that the couplings of the rate matrix are chosen to act inhibitory. Asymmetric inhibitory connections between different items are essential for the structural stability (see, for example, Ref. 20). The (spatial) interaction between the units is determined by the coupling matrix  $K$ :  $K_{k,l}$  is finite if unit  $l$  influences unit  $k$ , otherwise it is zero.

To compare the role of the attractor space in view of relaxation times, we consider GLV-equations with a possible nesting in the attractor space. One possibility to enforce nesting is to consider nine items and accordingly designed rate matrices. The rate matrix  $A$  is then chosen in such a way that the winnerless competition among its items has an attractor that is a (large) heteroclinic cycle (LHC) between three saddles that are themselves (small) heteroclinic cycles (SHCs) between three saddle equilibria [see Fig. 6(a)]. In this case, a kind of rock-paper-scissors game is played on two scales: between clusters of three items and within these clusters between three items each. As we have shown in Refs. 21 and 22, this structure of the attractor induces a hierarchy in time scales of slow oscillations (due to LHCs) modulating fast oscillations (due to SHCs), as experimentally observed in brain dynamics (see, for example, Refs. 23 and 24). The large (small) time scale amounts to one revolution in the large (small) heteroclinic cycle, respectively, which is well defined as long as the slowing down is suppressed by the application of a small amount of noise, otherwise it is itself a function of time.

The rate matrix  $A$  for the units with two hierarchy levels is then given as the following block matrix:

$$A = \begin{pmatrix} m_0 & m_d & m_f \\ m_f & m_0 & m_d \\ m_d & m_f & m_0 \end{pmatrix}, \text{ where } m_0 = \begin{pmatrix} 0 & c & e \\ e & 0 & c \\ c & e & 0 \end{pmatrix}. \quad (2)$$

Matrix  $m_d$  is also  $3 \times 3$  and has rates  $d$  on the diagonal elements and  $r$  on the remaining elements. Similarly, matrix  $m_f$  has a rate  $f$  on the diagonal with all off-diagonal elements being  $r$ . The rates characterize the “competition” strength in a winnerless game of items.

On tuning the decay rate  $\gamma$ , the system undergoes a sequence of Hopf bifurcations, whose order and values depend on the choice of the other parameters.<sup>21,22</sup> Two types of Hopf bifurcations are relevant in this context, which we here only summarize. For low values of  $\gamma$ , the system has an intricate heteroclinic dynamics with two hierarchy levels. When  $\gamma$  is increased toward a bifurcation point  $\gamma_{c1}$ , the system undergoes a Hopf bifurcation, at which the highest hierarchy level is gone. What remains is an LHC between three three-item saddle equilibria as a remnant of the SHCs. Further increasing  $\gamma$ , the system undergoes a second Hopf bifurcation at  $\gamma_{c2}$ , which drives the unit into stable global coexistence of nine items with the same concentrations. For further details of the bifurcation analysis, we refer to Refs. 21 and 22.

This means, we have to deal with a system that—depending on the value of  $\gamma$ —either performs slow oscillations of fast oscillations [two hierarchy levels, state (a)], or only fast oscillations [one hierarchy level, state (b)], or approaches a coexistence equilibrium of all included items. Before we apply the quench in  $\gamma$  toward the coexistence equilibrium, the system is prepared either in state (a) or in state (b).

Throughout this paper, we choose the parameters  $r = 1.25$ ,  $e = 0.2$ ,  $f = 1.3$ , and  $d = 2$ , for which the Hopf bifurcations of interest are at  $\gamma_{c1} = 1.1$  and  $\gamma_{c2} = 1.45$ . From the work of Ref. 25, we know that at  $\gamma_{c1} = 1.1$ , we observe the typical features of criticality with emerging long time scales in the dynamics. This feature will also have an impact on the relaxation of the HU.

In passing, we should remark that the very construction of the adjacency matrix  $A$  in phase space serves to enforce hierarchical heteroclinic motion just by the choice of rates, without additional equations and explicit implementation of different time scales as in Ref. 10, for example. The rates are chosen out of certain intervals so that the eigenvalues of the corresponding Jacobians at the saddle equilibria lead to a preference of the trajectory for one (desired) direction out of two unstable directions when escaping from the saddles. Our choice is just for convenience to generate an intricate structure in the attractor space by a single set of equations.

In extension of such a single hierarchical heteroclinic network, the dynamics on a spatial network (a two-dimensional square lattice) of identical such HUs was analyzed in Ref. 14, where the units were coupled via diffusion. Here, this extension serves for analyzing the impact of synchronization on relaxation. The set of Eq. (1) is then complemented by a grid Laplacian, with homogeneous diffusion constant  $\delta$ . Alternatively, in Ref. 26, we considered HUs along a chain, for which one unit acts as pacemaker with  $\gamma$  chosen from the regime of (nested) heteroclinic oscillations, while all other units are at rest in a coexistence equilibrium, and they can be entrained by the pacemaker. The coupling is directed or, if bidirectional, asymmetric with a weaker coupling back to the pacemaker.

In particular, for a system of two units and nine items, we consider one unit at location  $k = 1$  with decay rate  $\gamma_p$  acting as a pacemaker to the other (driven) unit at  $k = 2$  with decay rate  $\gamma_D$ .

The governing equation [Eq. (1)] takes then the following form:

$$\begin{aligned} \partial_t s_{1,i} &= \rho s_{1,i} - \gamma_p s_{1,i}^2 - \sum_{j \neq i} A_{ij} s_{1,i} s_{1,j} + \delta_b (s_{2,i} - s_{1,i}), \\ \partial_t s_{2,i} &= \rho s_{2,i} - \gamma_D s_{2,i}^2 - \sum_{j \neq i} A_{ij} s_{2,i} s_{2,j} + \delta (s_{1,i} - s_{2,i}), \end{aligned} \quad (3)$$

where we denote the interaction strength from the pacemaker to the driven unit, that is,  $K_{2,1}$ , by  $\delta$  and the back-coupling from the driven unit to the pacemaker ( $K_{1,2}$ ) by  $\delta_b$ . In this work, we consider  $\delta_b = 0.001$ . The components of  $A$  are given by Eq. (2).

For a longer chain, if we take one unit with nine items as the pacemaker and all other  $N - 1$  units as units at rest with unidirectional couplings, the unidirectional nearest-neighbor couplings along the chain are chosen according to the coupling matrix  $K$ , given as

$$K_{k,l} = \begin{cases} \delta & \text{if } k \in \{2, \dots, N\} \text{ and } l = k - 1, \\ 0 & \text{otherwise.} \end{cases}$$

We place a unit with two hierarchy levels as the pacemaker at the edge of the chain at  $k = 1$  with  $\gamma_1 = \gamma_p < 1.1$ . For all other units, we choose ( $\gamma_k = \gamma_D > 1.1 \forall k \in \{2, \dots, N\}$ ). Here, for  $k = 1$ , a small back-coupling from the  $N$ th node is added in analogy to the two units, i.e.,  $K_{1,N} = \delta_b = 0.001$ .

For further comparison and to stress the fact that it is not the mere number of items (or species in an ecological context) which makes a system complex, we consider another model with nine types of items, but with cyclic competition, no hierarchy in the attractor space and a single time scale of oscillations. It is given as

$$\partial_t s_i = \rho s_i - \gamma s_i^2 - s_i (c s_{i+1} + e s_{i+8}) \quad (4)$$

for  $i = 1, \dots, 9 \text{ mod } 9$ . The system has also a heteroclinic cycle but with six winners and three losers at a time and a stable coexistence equilibrium.

### III. RESULTS

#### A. A single hierarchical heteroclinic unit

We start with a single HHU with parameters chosen such that before the quench in  $\gamma$ , the system performs hierarchical heteroclinic oscillations with the characteristic slowing down as seen in Fig. 1(a). The slowing down is visible both in the increasing width of the blue, red, and green packages (chunks) of fast oscillations as well as within the chunks: The different shades of blue, red, and green trajectories display increasing times of revolutions within the (small) HCs. As to the large HC, the green chunk lasts longer than the red and the blue one, and the next blue (not displayed) would last longer than the green or the first blue one as the trajectory approaches the heteroclinic connections between the saddles.

The quench is realized from  $\gamma_1 = 1.05$  off the bifurcation point (which is at  $\gamma = 1.1$ ) to  $\gamma_2 = 1.55$  in the regime of item-coexistence, again off the second bifurcation point at  $\gamma = 1.45$ . For comparison, we start in Fig. 1(b) in a regime of a HC between three saddle equilibria, at which three items coexist at each of them at  $\gamma_1 = 1.3$  and also quench it to  $\gamma_2 = 1.55$  at  $t = 2000$ . Here, we have to deal with nine items but only one inherent time scale of oscillations.

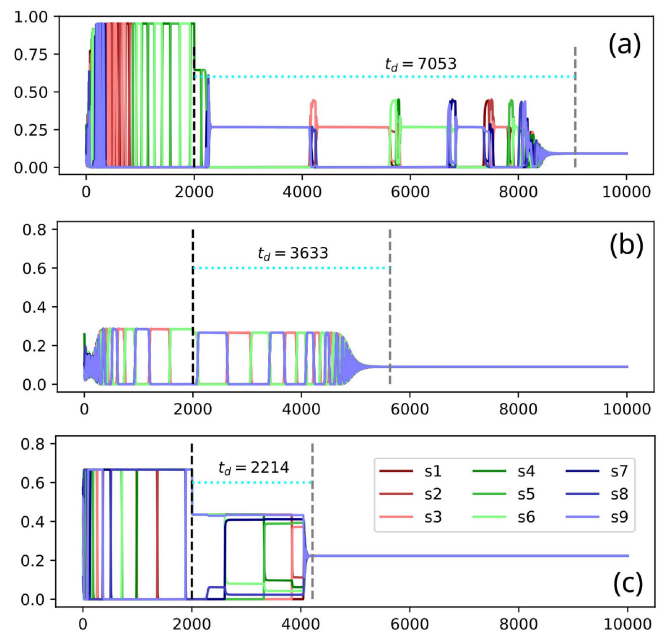


**FIG. 1.** Time evolution of nine items after a quench at  $t = 2000$  without noise. The black dashed lines mark the time when the quench is applied and the gray dashed lines correspond to the time when all variables go below the prescribed threshold ( $10^{-4}$ ). Panels (a) and (b): System described by Eqs. (1) and (2), starting the quench (a) from a regime of two hierarchy levels with  $\gamma_1 = 1.05$ , and (b) from one hierarchy level with  $\gamma_1 = 1.3$ , both to  $\gamma_2 = 1.55$ . Other parameters are  $c = 2.0, e = 0.2, d = 2.0, f = 0.3, r = 1.25$ , and  $\rho = 1$ . Panel (c) corresponds to a similar quench in the cyclic nine-item HU with one hierarchy level according to Eq. (4). For further explanations, see the text.

Alternatively in Fig. 1(c), we consider a system with nine items and only cyclic competition as in Eq. (4). For  $\gamma_1 = 1.5$ , the system shows heteroclinic motion with oscillations characterized by six temporary winners (rather than a single one) and three suppressed items at a time. This system is quenched to  $\gamma_2 = 2.5$ , which lies again in the regime of coexistence of nine items, off the bifurcation point.

In (a), the path of decay proceeds by passing saddles, which are the saddles at the new  $\gamma_2$ , these are the three three-item coexistence saddle equilibria, before it decays to the nine-item coexistence equilibrium. In (b) as well as in (c), the system directly starts from the new respective saddles at  $\gamma_2$  to the final nine-item coexistence equilibrium; here, the system still spends some time in the vicinity of the new saddles (under  $\gamma_2$ ), and the relaxation time for nine species (c) is shortest.

At the time of the quench, we observe in all cases a step in the amplitudes due to the shift in the saddle values before and after the quench. Obviously, the nesting of the attractor space in (a) together with the slowing down of the heteroclinic motion are essential for the long decay times. Apparently, there is no “short-cut” (heteroclinic connection) from the hierarchical heteroclinic motion directly to the coexistence equilibrium. Upon the decay, the system resolves the intermediate parameter regime. This is detailed in Fig. 2, which shows the values of the respective saddles before and after

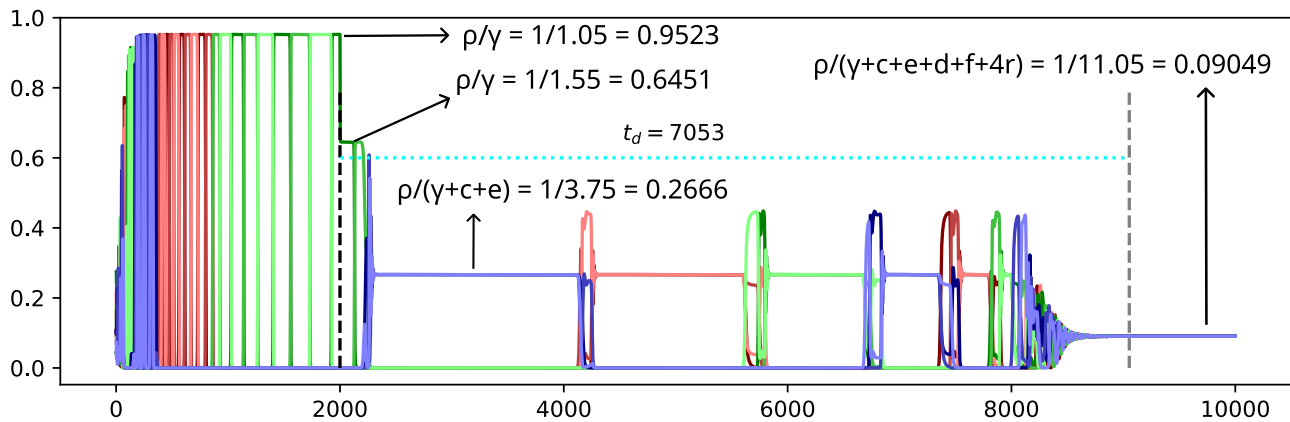


**FIG. 2.** Identification of the steps in the trajectories of the nine items while approaching the nine-item coexistence equilibrium. The steps are at the values of the saddles which the trajectories visit during decay on the itinerary through the HN after the quench at  $t = 2000$ .

the quench together with the coexistence equilibrium. For the one-item coexistence equilibrium, the coordinates are  $s_i = \rho/\gamma, s_j = 0$  for all  $j \neq i$ ; for the three-item coexistence saddles, they are  $s_i = s_{i+1} = s_{i+2} = \rho/(c + \gamma + e), s_j = 0$  for all  $j \notin \{i, i + 1, i + 2\}$  for  $i = 1, 4, 7$ ; and for the nine-item coexistence, saddle  $s_i = \rho/(c + \gamma + d + e + f + 4r)$ .

The qualitative features of the decay remain also true under the application of a small amount of noise such as  $\sigma = 10^{-13}$  in the corresponding panels of Fig. 3, though the slowing down of the heteroclinic motion is considerably reduced due to the noise and along with that the decay times in all three cases: from 7053 to 1264 in the respective panels (a), from 3633 to 1385 in panels (b), and from 2214 to 266 in panels (c). To analyze how representative the role of noise is in the plots of Fig. 3, we measure the decay time as a function of varying noise amplitude, but for 100 different initial conditions (Fig. 4) and vice versa, for one initial condition and 100 different noise realizations (not displayed).

The system is the nine-item hierarchical heteroclinic network for  $c = 2.0, e = 0.2, d = 2.0, f = 0.3, r = 1.25$ , and  $\rho = 1$ , and a quench at  $t = 2000$  from  $\gamma_1 = 1.05$  to  $\gamma_2 = 1.55$ . Each violin of the violin plot depicts the maximal, minimal, and mean value of the sampled runs, along with the distribution of values within this range. The mean values do not strongly depend on the noise amplitude, apart from  $\sigma = 10^{-5}$  for which the system does no longer see the heteroclinic attractor. The plot for 100 noise realizations looks very similar to the one in Fig. 4. The tendency is that noise considerably reduces the decay time. Obviously, a single HHU is sensitive both to varying initial conditions and to the very noise realization (not displayed).

So far, we considered a quench of bifurcation parameters  $\gamma$  from values off the bifurcation points at  $\gamma = 1.1$  and  $\gamma = 1.45$  to  $\gamma = 1.5$ , somewhere in between the respective regimes. How does the decay time depend on the size of the quench, starting or ending close to a bifurcation? Figure 5 shows the decay times in violin plots as a function of the destination point  $\gamma_2$  for 100 different noise realizations, and the plot for 100 different initial conditions looks very similar and is not displayed. As expected, the decay times diverge if

the quench is toward the immediate vicinity of the bifurcation point and further decay for larger  $\gamma_2$ ; the decay saturates to values almost independently of the initial conditions and the noise realizations when the quench is deep into the coexistence regime.

As a function of  $\gamma_1$ , the average decay time increases around the bifurcation point at  $\gamma_1 = 1.1$  to larger values in the regime of three

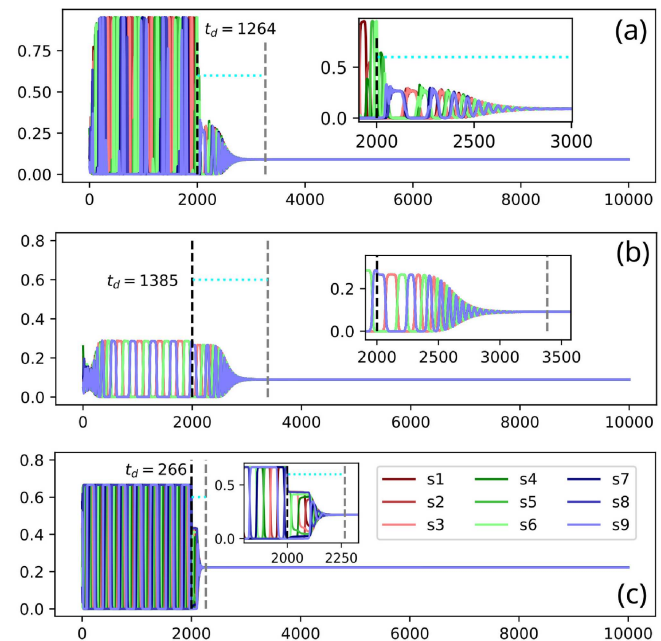


**FIG. 3.** Same as Fig. 1, but under the action of noise with amplitude  $\sigma = 10^{-13}$ . The relaxation time is considerably reduced. The decay after a quench from a regime with a HC between three three-species coexistence equilibria takes longer in (b) as compared to a quench from a regime with a HC between three HCs in (a). The shortest decay is for the system with cyclic competition.

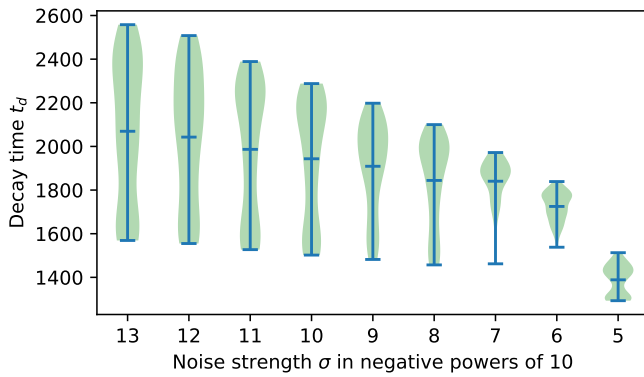


**FIG. 4.** Violin plot of the decay time as a function of the noise amplitude for 100 initial conditions and a single noise realization for a single HHU with  $c = 2.0, e = 0.2, d = 2.0, f = 0.3, r = 1.25, \rho = 1$  and a quench at  $t = 2000$  from  $\gamma_1 = 1.05$  to  $\gamma_2 = 1.55$ . The x axis denotes negative powers of 10.

three-item coexistence saddles, in agreement with the observations in Figs. 2(a) and 2(b) and, in contrast, to the case of no noise. Based on other observations (Figs. 6 and 7), this difference is attributed to a larger basin of attraction of the attractor with three three-item coexistence equilibria than the HC of HCs of Fig. 3(a) in the presence of noise.

**B. Two coupled heteroclinic units**

Next, we consider two coupled HUs, composed of one pacemaker with  $\gamma_1 = 1.05$  out of the regime of heteroclinic oscillations and one driven unit with  $\gamma_1 = 1.55$  out of the regime of the nine-item coexistence equilibrium, while the other parameters are chosen as before as  $c = 2.0, e = 0.2, d = 2.0, f = 0.3, r = 1.25$ , and  $\rho = 1$  with and without noise with an amplitude of  $\sigma = 10^{-13}$ . The coupling is directional with forward coupling  $\delta = 0.1$  and small backward coupling  $\delta_b = 0.001$ . The quench is from  $\gamma_1 = 1.05$  to  $\gamma_2 = 0.1.55$  at time  $t = 2000$ . We know from the work of Ref. 26

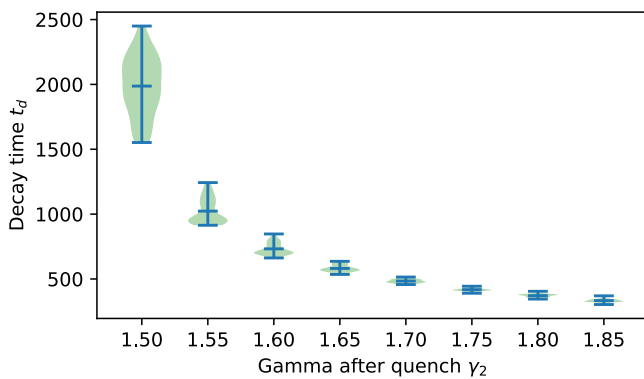


**FIG. 5.** Inertia as a function of the quench depth due to varying  $\gamma_2$  for the HHU for 100 noise realizations and one initial condition. The relaxation time is particularly large in the vicinity of the bifurcation point. Parameters are  $\sigma = 10^{-12}$ , otherwise as in Fig. 4, in particular,  $\gamma_1 = 1.05$ .

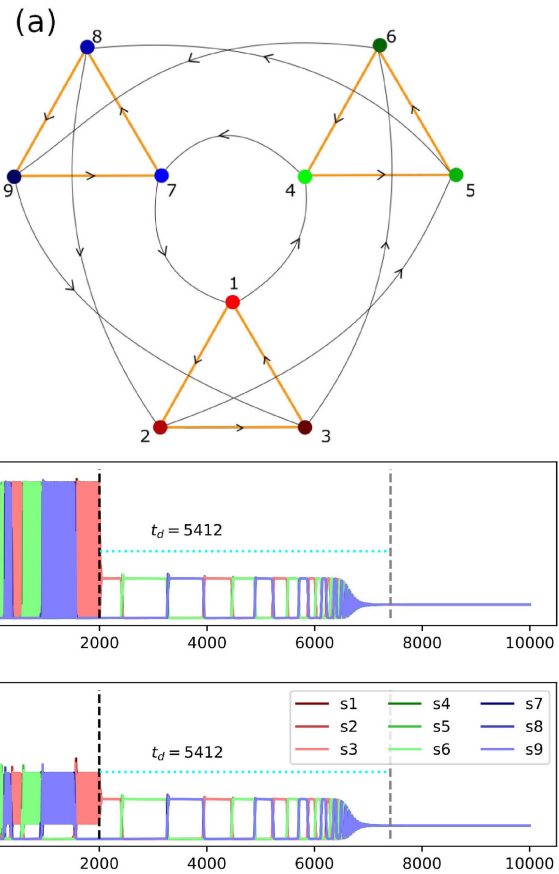


**FIG. 6.** (a) Schematic HHN with heteroclinic attractor  $(1, 2, 3) \rightarrow (6, 4, 5) \rightarrow (8, 9, 7)$ , iterative. (b) Pacemaker (HHU) choosing the path as indicated (a), coupled to a driven unit (c) with directed coupling. The driven unit gets entrained to the motion of the pacemaker with smaller amplitude oscillations, otherwise both units show the same relaxation times.

that this coupled system is at least bistable. Depending on the initial condition, the system chooses one of two possible itineraries in the HN, one with a large and one with a small basin of attraction. The itineraries differ by the order in which the nine saddles are passed by [see the corresponding panels (a) in Figs. 6 and 7]. Assigning a label to the nine saddles, from 100 different initial conditions 95 itineraries choose the first path, visiting the saddles  $(1, 2, 3) \rightarrow (6, 4, 5) \rightarrow (8, 9, 7)$ , while five initial conditions lead to the second path  $(1, 4, 7) \rightarrow (8, 2, 5) \rightarrow (6, 9, 3)$ .<sup>26</sup>

The main difference between the long lasting decays of the pacemaker's and the driven unit's trajectories is the amplitude of heteroclinic oscillations. Otherwise, the driven unit follows the pacemaker, and the decay time gets considerably reduced in the presence of noise from  $t_d = 5465$  (Fig. 6) to  $t_d = 1337$  (not displayed). These results hold for the itinerary in the heteroclinic network with the large basin of attraction.

If the initial conditions lead to a choice of heteroclinic trajectory in the HN that has a small basin of attraction (Fig. 7), the decay

01 November 2023 16:03:31

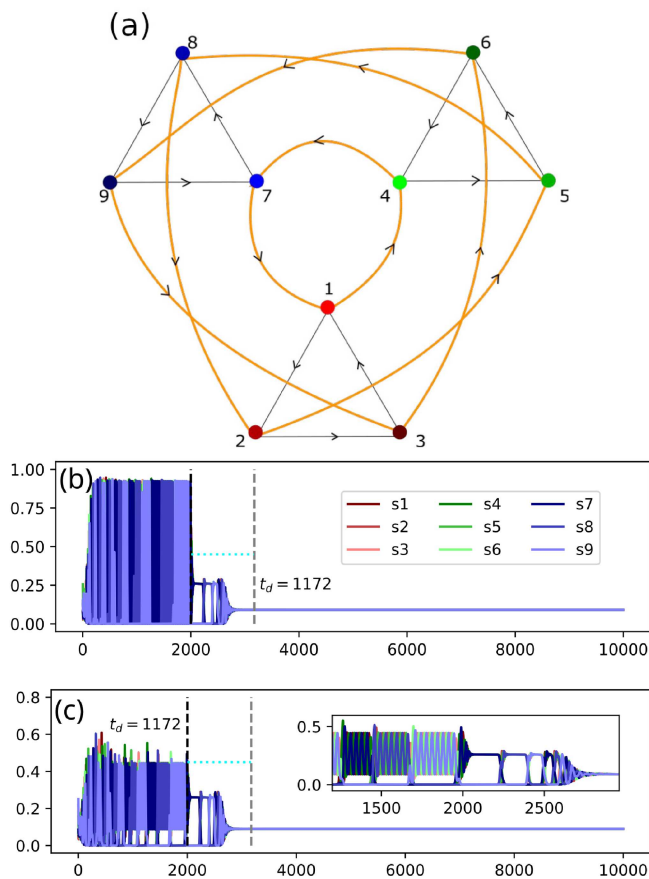


**FIG. 7.** Same as Fig. 6, but choosing the heteroclinic attractor (1,4,7)  $\rightarrow$  (8,2,5)  $\rightarrow$  (6,9,3), for which the decay time is considerably reduced along with the smaller size of the basin of attraction.

time is reduced as compared to the corresponding cases of Fig. 6. While it is more difficult for the itinerary to be captured by this basin, it is easier to escape toward to the coexistence equilibrium. Thus, the nesting of the attractor alone does not induce a long decay time, since for both paths, the respective attractors are nested. It is the size of the basin that matters.

The dependence of the decay time on the forward coupling is moderate. The violin plot of the decay time in Fig. 8 as a function of the coupling strength  $\delta$  shows a change in the bimodal distribution along the violins. For  $\delta \geq 0.3$ , the mean decay times are shorter. This may be due to the fact that for stronger coupling, the system behaves more like a single unit that is more sensitive to the very realization of noise than a weakly coupled system.

### C. Chain of a pacemaker with driven units

If we have to deal with a chain of one pacemaker and, for example, 15 driven units and consider a driven unit, for example, four

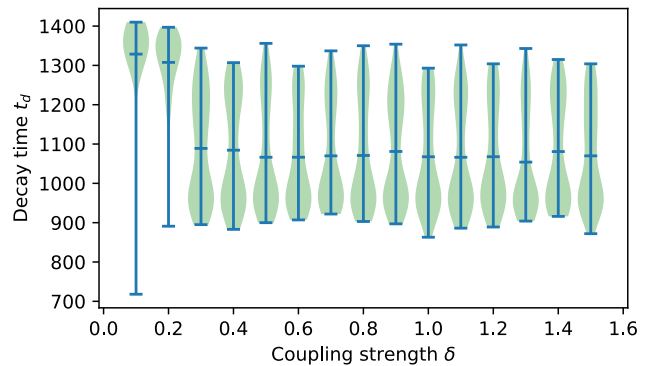


**FIG. 8.** Inertia as a function of the directed coupling  $\delta$  between pacemaker and driven units as a violin plot for 100 initial conditions and one noise realization. The bimodal distributions along the violins indicate that for  $\delta > 0.2$ , the decay starts preferably from the alternative path of Fig. 7, while smaller coupling seems to favor the path of Fig. 6.

sites apart from the pacemaker, the violins of the decay times indicate a reduced decay time for stronger noise both for 100 initial conditions and one noise realization and vice versa. For different initial conditions, the distributions along individual violins are bimodal due to the two basins of attraction of different size and accordingly different “escape times”; instead, the variation with the noise realization for one and the same initial condition is unimodal. The difference between the minimal and maximal values of the decay times for different noise realizations is much smaller than for a single unit. The results for this specific position along the chain are similar at other positions with the only difference in the amplitudes of the driven units which decrease with increasing distance to the pacemaker (not displayed).

Measuring the relaxation time as a function of the coupling strength along the chain, at a typical driven unit, say again at site 5, we see that it is independent of the coupling strength for a large range of couplings (Fig. 9), both for varying initial conditions or noise realizations, where the minimal decay times along all violins are due to the second heteroclinic attractor.

### D. Quench in two-dimensional synchronized grids

If we start from a  $20 \times 20$  system of HUs, coupled (bidirectionally) via diffusion and with uniformly chosen individual parameters, in particular, uniform  $\gamma_1 = 1.05$ , we know from the work of Ref. 14 that for sufficiently strong diffusion strength  $\delta$ , the entire grid synchronizes to the motion of a single HHU and flips in synchrony between the nine item types. Here, one may wonder how synchronization changes the relaxation, if the oscillations are stopped via a quench of the bifurcation parameter  $\gamma$  toward the coexistence regime, either via the one parameter in the single unit or via all 400  $\gamma$ s in the coupled system. In Fig. 10, we compare trajectories for the very same initial condition, no noise, of a single unit with trajectories of a typical node (0,0), representative for the  $20 \times 20$  grid, coupled with  $\delta = 0.5$ . Figure 10 shows that synchronization reduces the relaxation time. While the path toward the coexistence equilibrium is the same, the dwell times are reduced on the  $20 \times 20$  grid.



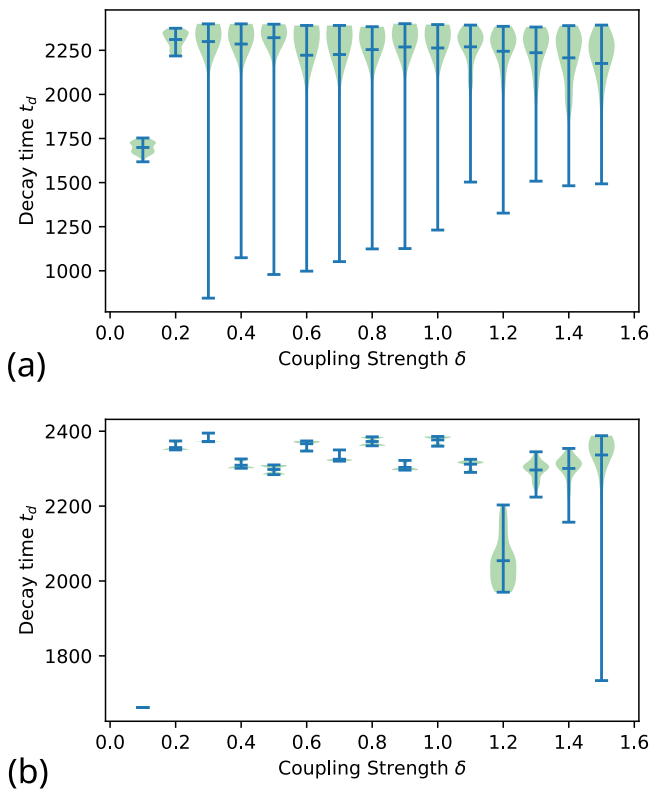


**FIG. 9.** Inertia of a driven unit within a ring of a pacemaker ( $\gamma_1 = 1.05$ , quenched to  $\gamma_2 = 1.55$  at  $t = 2000$ ) coupled to 15 driven units kept at ( $\gamma_1 = 1.55$ ), where the last driven unit of the chain is coupled to the pacemaker with a small back-coupling ( $\delta_b = 0.001$ ). The violin plots are for 100 initial conditions (a) and 100 noise realizations (b). Other parameters are  $c = 2.0$ ,  $e = 0.2$ ,  $d = 2.0$ ,  $f = 0.3$ ,  $r = 1.25$ ,  $\rho = 1$ , and  $\sigma = 10^{-13}$ . For further explanations, see the text.

Also for other coupling strengths ( $\delta = 0.7, 0.3, 0.1$ ), the relaxation time is shorter than for a single unit; thus, their synchronization accelerates the decay.

Further, we are interested in cases for which only a fraction of randomly selected units are quenched to the coexistence regime. In the presence of noise ( $\sigma = 10^{-13}$ ) and at time instant  $t = 2000$ , these are 10% in Fig. 11(a), 50% in Fig. 11(b), and 80% in Fig. 11(c). In (a), after a long decay period of the second hierarchy level, visible until roughly  $t = 3500$ , the units synchronize to small amplitude heteroclinic oscillations between the three three-item-coexistence equilibria. Also, in Fig. 11(b), the quench is not strong enough to stop the oscillations, but the units synchronize to oscillations with smaller amplitudes and at higher frequencies than in (a), while the oscillations stop toward the nine-item coexistence fixed point in Fig. 11(c), when 80% are quenched. The path in Fig. 11(c) is similar to that of Fig. 10(a), but the relaxation time is shorter due to the presence of noise and the absence of slowing down in Fig. 11(c).

The comparison between the different stationary states in Fig. 11 reveals that the fraction of units which are quenched to a

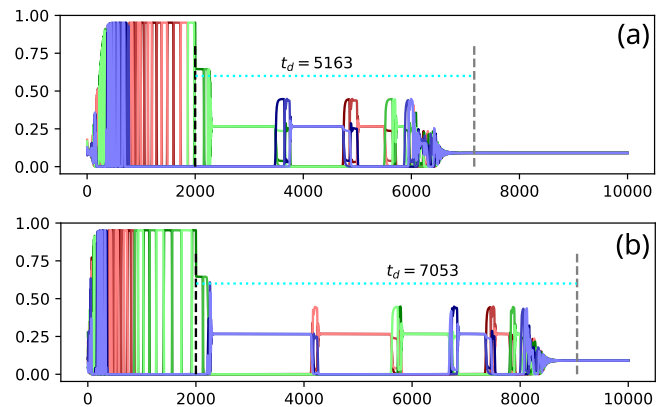


**FIG. 10.** Synchronization accelerates the decay or reduces the relaxation time. This is seen by a comparison between the decay time of a single HHU (b) to  $\gamma = 1.55$ , and the decay time of a typical node [here (0,0)] (a) toward the coexistence equilibrium; in (a) on a  $20 \times 20$  grid of identical HHUs, coupled with  $\delta = 0.5$ , and quenched at  $t = 2000$  for all units simultaneously toward  $\gamma = 1.55$ . All units are starting from the very same initial condition in both panels.

resting state may act as a control parameter for a variety of oscillatory synchronization patterns on the two-dimensional grid, in particular, patterns, which are typical for an intermediate parameter range of a single HHU such as in Fig. 11(a).

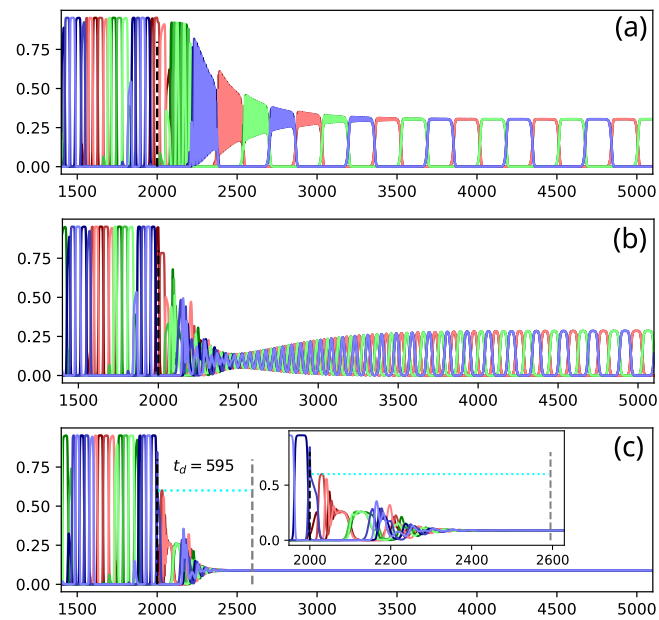


**FIG. 11.** Comparison between the effect of a quench of 10% (a), 50% (b), and 80% (c) of initially HHUs to the parameters of a nine-item coexistence equilibrium. Displayed are trajectories at individual sites of a fully synchronized grid, indicating different stationary states that are approached; oscillations are only arrested in case (c). Here, noise strength  $\sigma = 10^{-14}$ , coupling strength  $\delta = 0.5$  and the HHUs are quenched at  $t = 2000$  toward  $\gamma = 2.0$ .

#### IV. SUMMARY AND OUTLOOK

We have considered the relaxation times of heteroclinic motion under a quench in one of the bifurcation parameters from a regime of hierarchical heteroclinic oscillations to a coexistence equilibrium point. As a measure for the relaxation, we determined the time it takes after the quench to approach very small amplitude oscillations around the coexistence equilibrium point. Long relaxation times support the stability of the system in the sense that it is insensitive to perturbations on time scales shorter than the typical value of relaxation time. For a while, the system keeps some memory of the previous state. Fast relaxation, on the other hand, is useful for fast switching and adaptation to new system parameters.

As it turned out in our numerical simulations, slow relaxation is supported by a nesting attractor space if the quench is across different bifurcations and the path to escape proceeds along a number of saddles (here demonstrated for the case of a HHN with two hierarchy levels). Nesting alone is no guarantee for a long decay time, the basin of attraction of a nested attractor should be sufficiently large as well, as our two attracting paths within the same HHN have shown. As long as the only effect of noise is to suppress the slowing down of heteroclinic oscillations, it reduces the relaxation time as compared to the absence of noise. On the other hand, noise should not be too large to “blur” the structure of the heteroclinic attractor.

A pronounced dependence on the depth of the quench is only seen in the vicinity of the bifurcation region, both where the quench starts and where it ends. The sensitivity to initial conditions is weak, unless the system is multistable. The sensitivity to different noise realizations for one and the same noise strength is higher for a single HU than for a coupled system.

We considered two versions of couplings of HUs on a spatial grid. The first one was a configuration with a pacemaker and one or more driven units, which get entrained to the pacemaker motion once they are directed coupled. The second version was diffusive coupling between identical HUs with homogeneous parameters in an oscillatory regime. As to the pacemaker configurations, the relaxation was not sensitive to the distance of the driven units from the pacemaker, neither was there a clear dependence on the coupling strength.

For the second version, we started from a uniform set of HHUs, diffusively coupled and coupled strongly enough that the entire grid synchronizes to the dynamics of a single HHU. If this system is quenched in all individual constituents to the coexistence equilibrium, one may wonder whether the system remains sensitive to its composition even when it otherwise behaves like a single HHU. It remains sensitive, as it approaches the resting state faster if it is composed of many synchronized units and starts from such a state.

If instead we quench not all, but only a certain fraction of HHUs, the final state is fully synchronized, but oscillations are only arrested if the fraction of quenched units is sufficiently large. Also, the pattern of synchronization depends on this fraction.

Slow relaxation is obviously only one facet of stability of a complex system. The role of slow underdamped relaxations of heteroclinic motion resembles the role of inertia in power grids, both are measured in units of time, and large inertia in power grids is considered as one guarantor of grid stability (see, for example, Ref. 27). If we regard slow relaxation toward a new state as one criterion for stability, the answer to the question of whether stability increases or

decreases with increasing complexity is: it depends. A large number of items in a heteroclinic network alone neither makes the system more complex nor more fragile, as we have seen for the different versions of nine competing items; in particular, we observed a long lasting decay of the nested oscillations rather than an abrupt arrest, as if the system resists an enforced change of its current state, which raised our interest in this topic.

As an outlook, we speculate about possible applications of (slow) relaxation times in malfunction in brain dynamics. Heteroclinic cycles provide a possible explanation of various gaits in animal, human, and robot motion.<sup>28,29</sup> A typical symptom of Parkinson’s disease is the failure to stop motion like walking without delay, even if required from sensory input of obstacles in front. Moreover, it is known that neuromodulators like dopamine, serotonin, or GABA (gamma-aminobutyric acid) have an impact, in particular, on heteroclinic connections,<sup>30</sup> and that their functioning is affected in Parkinson’s disease. Therefore, we expect that an investigation of how to control relaxation times of heteroclinic dynamics deserves further attention also in view of explaining malfunction in brain dynamics.

#### ACKNOWLEDGMENTS

We would like to thank Bhumika Thakur (formerly at Jacobs University Bremen) for valuable discussions at the beginning of this work and the German Research Foundation (DFG, Contract No. ME-1332/28-2) for financial support. One of us (H.M.O.) is also indebted to Jürgen Kurths for including her in two larger collaboration projects CoNDyNet and CoNDyNet2 on power grids and valuable discussions therein.

#### AUTHOR DECLARATIONS

##### Conflict of Interest

The authors have no conflicts to disclose.

#### Author Contributions

**Hildegard Meyer-Ortmanns:** Conceptualization (lead); Funding acquisition (lead); Investigation (equal); Methodology (equal); Supervision (lead); Writing – original draft (lead); Writing – review & editing (lead). **Manoj Aravind:** Investigation (lead); Methodology (lead); Software (lead); Visualization (lead).

#### DATA AVAILABILITY

The data that support the findings of this study are available from the corresponding author upon reasonable request.

#### REFERENCES

- <sup>1</sup>V. Afraimovich, I. Tristan, R. Huerta, and M. I. Rabinovich, “Winnerless competition principle and prediction of the transient dynamics in a Lotka–Volterra model,” *Chaos* **18**, 043103 (2008).
- <sup>2</sup>F. H. Busse and K. Heikes, “Convection in a rotating layer: A simple case of turbulence,” *Science* **208**, 173–175 (1980).
- <sup>3</sup>A. Szolnoki, M. Mobilia, L.-L. Jiang, B. Szczesny, A. M. Rucklidge, and M. Perc, “Cyclic dominance in evolutionary games: A review,” *J. R. Soc. Interface* **11**, 20140735 (2014).

- <sup>4</sup>M. A. Nowak and K. Sigmund, “Bacterial game dynamics,” *Nature* **418**, 138–139 (2002).
- <sup>5</sup>M. I. Rabinovich, V. S. Afraimovich, C. Bick, and P. Varona, “Information flow dynamics in the brain,” *Phys. Life Rev.* **9**, 51–73 (2012).
- <sup>6</sup>V. Afraimovich, X. Gong, and M. Rabinovich, “Sequential memory: Binding dynamics,” *Chaos* **25**, 103118 (2015).
- <sup>7</sup>M. I. Rabinovich, I. Tristan, and P. Varona, “Hierarchical nonlinear dynamics of human attention,” *Neurosci. Biobehav. Rev.* **55**, 18–35 (2015).
- <sup>8</sup>P. Varona and M. I. Rabinovich, “Hierarchical dynamics of informational patterns and decision-making,” *Proc. R. Soc. B: Biol. Sci.* **283**, 20160475 (2016).
- <sup>9</sup>M. I. Rabinovich, V. S. Afraimovich, and P. Varona, “Heteroclinic binding,” *Dyn. Syst.* **25**, 433–442 (2010).
- <sup>10</sup>M. I. Rabinovich, P. Varona, I. Tristan, and V. S. Afraimovich, “Chunking dynamics: Heteroclinics in mind,” *Front. Comput. Neurosci.* **8**, 22 (2014).
- <sup>11</sup>V. Kirk and M. Silber, “A competition between heteroclinic cycles,” *Nonlinearity* **7**, 1605 (1994).
- <sup>12</sup>P. Ashwin and M. Field, “Heteroclinic networks in coupled cell systems,” *Arch. Ration. Mech. Anal.* **148**, 107–143 (1999).
- <sup>13</sup>P. Ashwin and C. Postlethwaite, “Designing heteroclinic and excitable networks in phase space using two populations of coupled cells,” *J. Nonlinear Sci.* **26**, 345–364 (2016).
- <sup>14</sup>M. Voit and H. Meyer-Ortmanns, “Dynamics of nested, self-similar winnerless competition in time and space,” *Phys. Rev. Res.* **1**, 023008 (2019).
- <sup>15</sup>E. Tognoli and J. S. Kelso, “The metastable brain,” *Neuron* **81**, 35–48 (2014).
- <sup>16</sup>M. I. Rabinovich, R. Huerta, P. Varona, and V. S. Afraimovich, “Generation and reshaping of sequences in neural systems,” *Biol. Cybern.* **95**, 519–536 (2006).
- <sup>17</sup>M. I. Rabinovich and P. Varona, “Robust transient dynamics and brain functions,” *Front. Comput. Neurosci.* **5**, 24 (2011).
- <sup>18</sup>M. I. Rabinovich and M. Muezzinoglu, “Nonlinear dynamics of the brain: Emotion and cognition,” *Phys.-Usp.* **53**, 357 (2010).
- <sup>19</sup>M. I. Rabinovich, M. A. Zaks, and P. Varona, “Sequential dynamics of complex networks in mind: Consciousness and creativity,” *Phys. Rep.* **883**, 1–32 (2020).
- <sup>20</sup>V. S. Afraimovich, T. R. Young, and M. I. Rabinovich, “Hierarchical heteroclinics in dynamical model of cognitive processes: Chunking,” *Int. J. Bifurcation Chaos* **24**, 1450132 (2014).
- <sup>21</sup>M. Voit and H. Meyer-Ortmanns, “A hierarchical heteroclinic network: Controlling the time evolution along its paths,” *Eur. Phys. J. Spec. Top.* **227**, 1101–1115 (2018).
- <sup>22</sup>M. Voit and H. Meyer-Ortmanns, “Predicting the separation of time scales in a heteroclinic network,” *Appl. Math. Nonlinear Sci.* **4**, 279–288 (2019).
- <sup>23</sup>M. Mölle and J. Born, “Slow oscillations orchestrating fast oscillations and memory consolidation,” *Prog. Brain Res.* **193**, 93–110 (2011).
- <sup>24</sup>M. Saleh, J. Reimer, R. Penn, C. L. Ojakangas, and N. G. Hatsopoulos, “Fast and slow oscillations in human primary motor cortex predict oncoming behaviorally relevant cues,” *Neuron* **65**, 461–471 (2010).
- <sup>25</sup>M. Voit and H. Meyer-Ortmanns, “Emerging criticality at bifurcation points in heteroclinic dynamics,” *Phys. Rev. Res.* **2**, 043097 (2020).
- <sup>26</sup>B. Thakur and H. Meyer-Ortmanns, “Heteroclinic units acting as pacemakers: Entrained dynamics for cognitive processes,” *J. Phys.: Complex.* **3**, 035003 (2022).
- <sup>27</sup>D. Witthaut, F. Hellmann, J. Kurths, S. Kettmann, H. Meyer-Ortmanns, and M. Timme, “Collective nonlinear dynamics and self-organization in decentralized power grids,” *Rev. Mod. Phys.* **94**, 015005 (2022).
- <sup>28</sup>T. Brecej and T. Petrič, “Stable heteroclinic channel networks for physical human–humanoid robot collaboration,” *Sensors* **23**, 1396 (2023).
- <sup>29</sup>M. Golubitsky, I. Stewart, P.-L. Buono, and J. Collins, “Symmetry in locomotor central pattern generators and animal gaits,” *Nature* **401**, 693–695 (1999).
- <sup>30</sup>K. M. Shaw, D. N. Lyttle, J. P. Gill, M. J. Cullins, J. M. McManus, H. Lu, P. J. Thomas, and H. J. Chiel, “The significance of dynamical architecture for adaptive responses to mechanical loads during rhythmic behavior,” *J. Comput. Neurosci.* **38**, 25–51 (2015).